

# Structural elucidation and study of intermolecular interactions in *meso*-tetratolylporphyrins

Rahul Soman, Subramaniam Sujatha and Chellaiah Arunkumar\*

Bioinorganic Materials Research Laboratory, Department of Chemistry, National Institute of Technology Calicut, Kozhikode, Kerala 673 601, India

Received 8 April 2016

Accepted 3 June 2016

**ABSTRACT:** Synthesis and crystal structure analysis of *meso*-tetratolylporphyrins, **1–5** combined with computational Hirshfeld surface analysis were investigated. The crystal packing of porphyrins **1, 3** and **4** are arranged in an “orthogonal fashion” whereas **2** and **5** are in a “slip-stack or off-set fashion” through various intermolecular interactions. Compound **2** exhibits saddle geometry whereas **5** showed a domed geometry as evident from the single crystal X-ray diffraction studies. The enhancement of non-planarity in **2** is probably due to the presence of numerous intermolecular interactions caused by the presence of trifluoroacetate anions on both faces of the porphyrin in addition to the bulky bromine groups at the  $\beta$ -pyrrole positions. In **5**, the non-planarity is merely due to the metal coordination at the porphyrin core as pentacoordinated  $Mn^{III}$  center with a chloro ligand in the axial position. Hirshfeld surface analysis was performed in order to analyze the various intermolecular interactions present in these porphyrins and the result was discussed.

**KEYWORDS:** tolylporphyrins, non-planar porphyrins, crystal structure analysis, Hirshfeld surface analysis, intermolecular interactions.

## INTRODUCTION

Porphyrins are tetra-pyrrolic, highly colored pigments and nature has chosen them for the biological functions such as electron transfer, oxygen transport, photosynthesis energy transduction, *etc.*, because of their highly flexible skeleton which allows a range of distorted non-planar conformations [1, 2]. The distorted conformations are ubiquitous in the hemes of hemoproteins, the pigments of photosynthetic proteins and cofactor F430 of methylreductase. The introduction of substituents at the  $\beta$ -pyrrole position leads to distortion of the porphyrin core from planarity due to steric repulsion and these non-planar conformations are employed as models for naturally available tetrapyrrolic pigments [3]. In particular, distorted porphyrins with sterically hindered electron withdrawing substituents are employed to mimic the catalytic activity of cytochrome

P-450 [4]. It is well-known that the  $\beta$ -halogenated non-planar porphyrin macrocycle shows remarkable bathochromic shift with smaller extinction coefficient compared planar analogs [4]. Theoretical studies reveal that the major cause for the red shift is due to nonplanarity-induced destabilization of the porphyrin HOMOs [5]. Insertion of small metal ion at the porphyrin core results in substantial changes in the degree of non-planarity, conformational flexibility and electron density distribution. It is also possible to induce the non-planarity in planar porphyrins by core modification, ring reduction/oxidation and by crystal packing effects. Among the various types of non-planar conformations of the porphyrin macrocycle, the most common distortions are the ruffling ( $B_{1u}$ ) and saddling ( $B_{2u}$ ) conformations in addition to the doming ( $A_{2u}$ ), waving ( $E_g$ ) and propeller ( $A_{1u}$ ) structures [6]. The dome structure is usually seen in metalloporphyrins possessing an axial fifth ligand. There has been a growing interest in the study of synthetic non-planar porphyrins to better understand the biological role of non-planar heme prosthetic groups

\*Correspondence to: Chellaiah Arunkumar, email: arunkumarc@nitc.ac.in, tel: +91 495-228-5307, fax: +91 495-228-7250

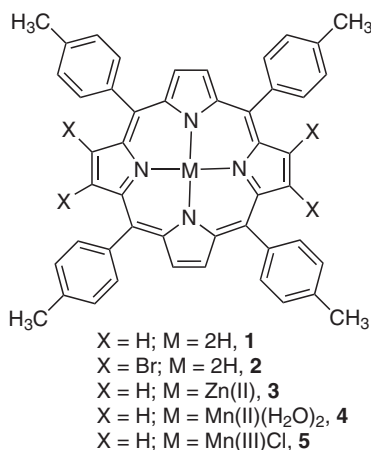


**Fig. 1.** Molecular structure of *meso*-tetratolylporphyrins under study

present in biomolecules. The first example of a sterically ruffled porphyrin bearing *meso*-substituents was reported by Senge *et al.* [7]. The non-planar porphyrins generally exhibit more intermolecular interactions compared to their planar analogs which control their structure and in turn the functional properties. Recently, we reported the intermolecular interactions of planar and non-planar fluorinated porphyrins bearing different *meso*-substituents [8]. Here, we report the synthesis and the detailed crystal structure analysis of few planar and non-planar *meso*-tetratolylporphyrins (Fig. 1) and their structural features are compared.

## RESULTS AND DISCUSSION

### Optical properties

5,10,15,20-Tetratolylporphyrin, H<sub>2</sub>TTP ligand, **1**, 2,3-,12,13-tetrabromo-5,10,15,20-tetratolylporphyrin, H<sub>2</sub>TTPBr<sub>4</sub> ligand, **2** were synthesized using the method reported by Lindsey *et al.* [9] and Bhyrappa *et al.* [10] respectively and the metal complexes, **3–5** were prepared by the literature method [11] to afford the desired complexes (Scheme 1).

The UV-visible spectra of porphyrins, **1** and **2** are very well matched with the reported H<sub>2</sub>TPP and H<sub>2</sub>TPPBr<sub>4</sub> [10] exhibiting the characteristic Soret and Q-bands. Notably, upon bromination of **1** to form **2**, it is noted that there is a reduction in the number of Q-bands from 4 to 3 as observed in H<sub>2</sub>TPPBr<sub>4</sub>. The overlaid spectra for H<sub>2</sub>TPP and H<sub>2</sub>TPPBr<sub>4</sub> and **1** and **2** was made and portrayed in Figs 2a and 2b respectively.

As seen from Fig. 2b, the Soret band of the antipodal brominated product of H<sub>2</sub>TTP shows red shifted absorption spectrum of 19 nm, similar to brominated H<sub>2</sub>TPP (Fig. 2a) which confirms the formation of tetrabrominated product of **2**.

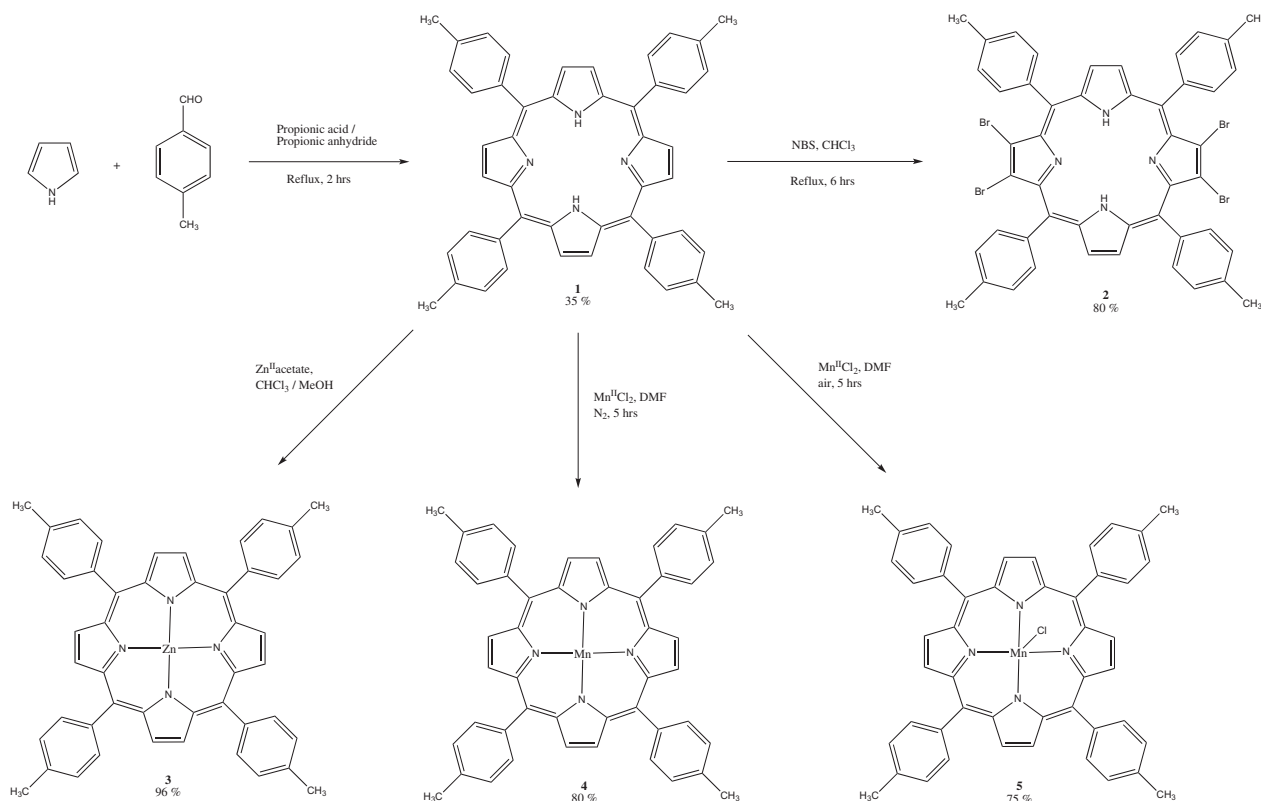
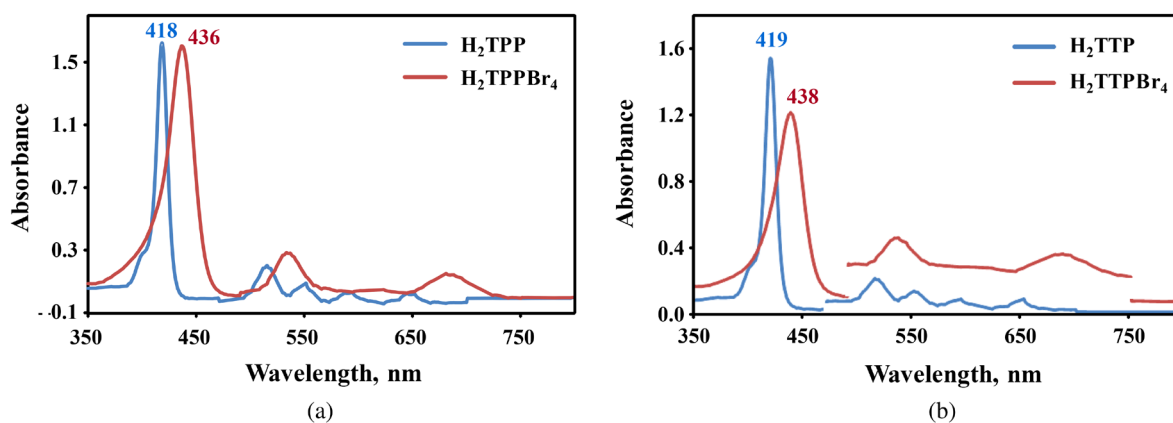
### Structural characterization by single crystal X-ray diffraction studies

Synthesis of tolylporphyrins, H<sub>2</sub>TTP, **1**; [H<sub>4</sub>TTPBr<sub>4</sub><sup>2+</sup>(CF<sub>3</sub>COO<sup>-</sup>)<sub>2</sub>(C<sub>2</sub>H<sub>4</sub>Cl<sub>2</sub>)], **2**; Zn<sup>II</sup>TTP, **3**; Mn<sup>II</sup>TTP (H<sub>2</sub>O)<sub>2</sub>, **4** and Mn<sup>III</sup>TTPCl, **5** is reported and are structurally characterized by single crystal X-ray diffraction analysis. Compounds, **1–4** are crystallized in monoclinic system with space groups, *P2<sub>1</sub>/c*, *P2<sub>1</sub>/n*, *C2/c* and *P2<sub>1</sub>/n* respectively, whereas **5** in triclinic with *P-1* (Table 1). The ORTEP and molecular crystal packing diagrams for compounds, **1–5** are shown in Figs 3–7.

The ORTEP diagrams of compound **1** show a planar arrangement of the porphyrin core (Figs 3a and 3b) and the molecular crystal packing is through the formation of “orthogonal arrangement” of molecules or  $\pi$ - $\pi$  stacking lead to form a one dimensional array (Fig. 4b) involving <sup>(ph)</sup>C–H...C<sup>(ph)</sup> and <sup>(methyl)</sup>C–H...N<sub>(pyr)</sub> interactions (Table 2). The diprotonated form of antipodal tetrabrominated compound, **2** [H<sub>4</sub>TTPBr<sub>4</sub><sup>2+</sup>(CF<sub>3</sub>COO<sup>-</sup>)<sub>2</sub>(C<sub>2</sub>H<sub>4</sub>Cl<sub>2</sub>)] is found to be *non-planar*, exhibits saddle geometry (Figs 3c and 3d) and the average mean plane deviation of the  $\beta$ -pyrrole and *meso*-carbon atoms are found to be  $\pm 1.1378(2)$  Å and  $\pm 0.0410(2)$  Å respectively, which is much greater than that of the reported tetrabrominated freebase 4-butoxyphenyl porphyrin, [12] ( $\pm 0.50(3)$  Å and  $\pm 0.038(3)$  Å). The enhanced non-planarity observed in **2** indicates that there is an effective interaction between the CF<sub>3</sub>COO<sup>-</sup> counter anions and porphyrin core due to their close proximity involving various intermolecular interactions. Moreover, the presence of two CF<sub>3</sub>COO<sup>-</sup> anions on both faces of the porphyrin core leads to diacid formation that enhances the non-planar nature of the porphyrin in addition to the bulky substituent present at the  $\beta$ -pyrrole positions.

Furthermore, the molecular crystal packing of **2** forms a “slip-stack or off-set arrangement” of molecules which is presumably due to the non-planarity of the core and hence there is no effective  $\pi$ - $\pi$  stacking observed which is depicted in Fig. 4c involving several intermolecular interactions, *viz.*, N–H...O, N–H...C, C–H...O, C–H... $\pi$ , C–H...N, Br...O, Br...Br, *etc.* (Table 2). Moreover, the intermolecular interactions in **2** were found to be mainly of hydrogen bonding between the oxygen atom of the CF<sub>3</sub>COO<sup>-</sup> anions and imino hydrogen of the porphyrin core and they are very strong owing to their close proximity; they found on both faces of the porphyrin core and in the range of 2.501–2.684 Å (Fig. 4a).

In **3**, the zinc(II) centre is tetra coordinated with the porphyrin core nitrogens, forms a square planar arrangement and the porphyrin core is found to be planar without any distortions (Figs 5a and 5b). The crystal packing diagram of **3** is in a “zigzag arrangement” of molecules formed through mainly of <sup>(ph)</sup>C–H...C<sup>(ph)</sup> and <sup>(ph)</sup>C...C<sup>(ph)</sup> interactions (Fig. 5c). The average Zn–N and Zn–C<sub>meso</sub> distances in **3** are 2.030(2) Å and 3.442(2) Å respectively which are comparable with the reported zinc(II)-*meso*-tetra(4-tolyl)porphyrins [13] (2.037(5), 2.036(18) Å and

Scheme 1. Synthesis of *meso*-tetratolyl porphyrinsFig. 2. Overlaid UV-visible spectra of porphyrins, (a)  $H_2TPP$  and  $H_2TPPBr_4$ ; (b)  $H_2TTP$ , **1** and  $H_2TPPBr_4$ , **2** in  $CH_2Cl_2$  ( $6.66 \times 10^{-6}$  M) at 298 K

3.444, 3.449 Å) as well as the four coordinate  $ZnTPP$  [14] (2.037(2) Å and 3.447 Å); whereas the average  $Zn-N$  distance is less than that of five- and six-coordinate  $Zn^{II}$  complexes (2.052(4) and 2.057(4) Å) [15].

Another set of planar and non-planar porphyrins in the present study is **4** (hexacoordinated  $Mn^{II}$ ) and **5** (pentacoordinated  $Mn^{III}$ ), which are differing each other by simple metal coordination at the porphyrin core.

In **4**, the water molecules are present in the apex positions which make the  $Mn^{II}$  ion to fit well into the

porphyrin core and the core is found to be planar in nature (Figs 6a and 6b). Like **1**, the crystal packing of **4** also exhibits “orthogonal arrangement” of molecules through  $(ph)C-H \cdots C(ph)$  interaction forming well-stabilized one dimensional array (Fig. 7a).

Due to the presence of an axial ligand (chloro) in **5**, the porphyrin core is domed in nature and it is slightly deviated from its planarity, the average mean plane displacement is  $\pm 0.2963(3)$  Å (Fig. 6d). The crystal packing in **5** is seen as “slip-stack or off-set fashion” as

**Table 1.** Crystal structure data of porphyrins under study, **1**, H<sub>2</sub>TTP; **2**, H<sub>4</sub>TTPBr<sub>4</sub><sup>2+</sup> (CF<sub>3</sub>COO<sup>-</sup>)<sub>2</sub> (C<sub>2</sub>H<sub>4</sub>Cl<sub>2</sub>); **3**, Zn<sup>II</sup>TTP; **4**, Mn<sup>II</sup>TTP (H<sub>2</sub>O)<sub>2</sub>; **5**, Mn<sup>III</sup>TTPCl

	H <sub>2</sub> TTP, <b>1</b>	H <sub>4</sub> TTPBr <sub>4</sub> (CF <sub>3</sub> COO <sup>-</sup> ) <sub>2</sub> (C <sub>2</sub> H <sub>4</sub> Cl <sub>2</sub> ), <b>2</b>	Zn <sup>II</sup> TTP, <b>3</b>	Mn <sup>II</sup> TTP (H <sub>2</sub> O) <sub>2</sub> , <b>4</b>	Mn <sup>III</sup> TTPCl, <b>5</b>
Formula	C <sub>48</sub> H <sub>38</sub> N <sub>4</sub>	C <sub>54</sub> H <sub>40</sub> Br <sub>4</sub> Cl <sub>2</sub> F <sub>6</sub> N <sub>4</sub> O <sub>4</sub>	C <sub>48</sub> H <sub>36</sub> N <sub>4</sub> Zn	C <sub>48</sub> H <sub>40</sub> MnN <sub>4</sub> O <sub>2</sub>	C <sub>49</sub> H <sub>38</sub> Cl <sub>2</sub> MnN <sub>4</sub>
CCDC	1041763	956522	1058016	1041764	980778
Crystal system	Monoclinic	Monoclinic	Monoclinic	Monoclinic	Triclinic
Space group	P2 <sub>1</sub> /c	P2 <sub>1</sub> /n	C2/c	P2/n	P-1
Colour	Purple	Dark green	Pink	Dark green	Dark green
a, Å	9.9183 (9)	15.4215 (7)	32.2573 (19)	14.0459 (13)	11.1373 (5)
b, Å	9.1489 (9)	15.1724 (7)	9.5520 (6)	9.9081 (10)	13.1844 (8)
c, Å	21.407 (2)	25.5568 (12)	14.9758 (8)	18.9491 (16)	28.0681 (16)
α, (deg)	90	90	90	90	82.437 (2)
β, (deg)	107.136 (6)	94.377 (2)	112.373 (5)	96.228 (4)	86.787 (2)
γ, (deg)	90	90	90	90	81.002 (2)
Volume, Å <sup>3</sup>	1856.2 (3)	5962.4 (2)	4267.0 (4)	2621.5 (4)	4032.7 (4)
Z	2	4	4	2	4
D <sub>calcd</sub> , mg/m <sup>3</sup>	1.200	1.463	1.143	0.963	1.332
λ, Å	0.71073	0.71073	0.71073	0.71073	0.71073
T, K	296 (2)	296 (2)	296 (2)	296 (2)	296 (2)
No. of unique reflections	3248	10285	3753	4603	14096
No. of parameters refined	241	712	244	253	1046
GOF on F <sup>2</sup>	1.015	1.031	1.033	1.030	1.002
R <sub>1</sub> <sup>a</sup>	0.0630	0.0629	0.0415	0.0738	0.0529
wR <sub>2</sub> <sup>b</sup>	0.1717	0.1754	0.1156	0.2176	0.1326

$$^a R_1 = \sum ||F_o| - |F_c|| / \sum |F_o|; I_o > 2\sigma(I_o). \quad ^b wR_2 = [\sum w(F_o^2 - F_c^2)^2 / \sum w(F_o^2)]^{1/2}.$$

observed in the case of non-planar porphyrin **2** molecule that indicates the less effective interactions between the porphyrin molecules.

Overall, the planar porphyrins, **1**, **3** and **4** possess similar kind of intermolecular interactions and they are stabilized mainly of the type of  $\text{C}_{(\text{ph})} \cdots \text{C}_{(\text{ph})}$  contacts which is in the range of 2.81 Å and the packing of molecules are in the “orthogonal fashion”; whereas in the case of non-planar porphyrins of **2** and **5**, the molecules are arranged in a “slip-stack or off-set fashion” through various intermolecular interactions.

### Study of intermolecular interactions

To analyze and quantify the various non-covalent interactions present in the crystal packing of planar and non-planar porphyrins (**1–5**), Hirshfeld surface (HS) analysis have been carried out using *Crystal Explorer 3.1* [16]. The HSs mapped with  $d_{\text{norm}}$  for the planar porphyrin **1** show the  $\text{C}_{(\text{methyl})} \cdots \text{N}_{(\text{pyr})}$  close contact with small red spots whereas its non-planar counterpart shows several red spots such as faint one for C $\cdots$ H close contact,

medium intense red spots for O $\cdots$ H close contact and big intense red spot for O $\cdots$ Br close contacts (Figs 8a–8e). Similarly, in the HS of planar manganese porphyrin **4**, only the C $\cdots$ H close contact is seen as small red spot whereas its non-planar analog **5** shows several medium intense red spots for H $\cdots$ H close contacts and faint red spots for C $\cdots$ H close contacts. Also, the planar zinc(II) porphyrin **3** shows only the C $\cdots$ H close contacts as small red spots. These results indicate that the non-planar porphyrins **2** and **5** exhibit several strong intermolecular interactions compared to the planar analogs.

The 2D fingerprint plots (FPs) of **1–5** indicating different inter-atomic interactions present in these crystals are shown in Figs 8f–8j. In planar porphyrins, the major contribution comes from the C $\cdots$ H [28% in **1**; 26% in **3**; 12% in **4**], and H $\cdots$ H [64% in **1**; 48% in **3**; 52% in **4**] contacts whereas in the case of non-planar porphyrins, apart from the major interactions detailed above, the interactions involving halogens of the solvent molecule are also observed (Fig. 9). In **2**, H $\cdots$ F/Cl/Br interaction accounts 24% and in **5** the H $\cdots$ Cl contact accounts 15%. The distribution of individual intermolecular interactions

**Table 2.** Distances (in Å) for the different types of interactions in the crystal packing of porphyrins, **1–5**

Interactions <sup>a</sup>	<b>1</b> <sup>b</sup>	<b>2</b> <sup>b</sup>	<b>3</b> <sup>b</sup>	<b>4</b> <sup>b</sup>	<b>5</b> <sup>b</sup>
(ph)C–H...C <sub>(ph)</sub>	2.881 (4)	—	2.750 (4)	2.808 (4)	—
(ph)C–H...C <sub>(β-pyr)</sub>	—	—	—	—	2.837–2.874 (4)
(ph)C–H...C <sub>(methyl)</sub>	—	—	—	—	2.855 (2)
(methyl)C–H...C <sub>(β-pyr)</sub>	—	—	—	—	2.875 (2)
(methyl)C–H...C <sub>(ph)</sub>	—	—	—	—	2.850–2.861 (4)
(methyl)C–H...C <sub>(methyl)</sub>	—	—	—	—	2.795–2.827 (4)
(ph)C–H...C <sub>(ph)</sub>	—	—	—	—	2.803–2.855 (4)
(β-pyr)C–H...C <sub>(ph)</sub>	—	2.781–2.820 (6)	—	—	—
(methyl)C–H...N <sub>(pyr)</sub>	2.704 (4)	—	—	—	—
(ph)C...C <sub>(ph)</sub>	—	—	3.334 (2)	—	—
(methyl)C...C <sub>(methyl)</sub>	—	—	—	—	3.395 (2)
(β-pyr)C...M <sub>(Mn)</sub>	—	—	—	—	3.644 (2)
(ph)C–H...O <sub>(CF<sub>3</sub>COO<sup>-</sup>)</sub>	—	2.565–2.684 (4)	—	—	—
(methyl)C–H...O <sub>(CF<sub>3</sub>COO<sup>-</sup>)</sub>	—	2.501 (1)	—	—	—
(β-pyr)N–H...O <sub>(CF<sub>3</sub>COO<sup>-</sup>)</sub>	—	1.776–1.870 (4)	—	—	—
(β-pyr)N–H...C <sub>(CF<sub>3</sub>COO<sup>-</sup>)</sub>	—	2.760–2.785 (4)	—	—	—
(ph)C–H...F <sub>(ph)</sub>	—	2.533 (2)	—	—	—
(methyl)C–H...F <sub>(ph)</sub>	—	2.627 (2)	—	—	—
(ph)C...F <sub>(ph)</sub>	—	3.068 (2)	—	—	—
(β-pyr)H...H <sub>(β-pyr)</sub>	—	—	—	—	2.203 (2)
(ph)H...H <sub>(ph)</sub>	—	2.368 (2)	—	—	2.165–2.199 (3)
(methyl)H...H <sub>(ph)</sub>	—	—	—	—	2.181–2.248 (4)
(β-pyr)C–Br...O <sub>(CF<sub>3</sub>COO<sup>-</sup>)</sub>	—	3.090–3.110 (4)	—	—	—
Br...Br	—	3.090 (2)	—	—	—
(β-pyr)N...O <sub>(CF<sub>3</sub>COO<sup>-</sup>)</sub>	—	2.657–2.914 (6)	—	—	—

<sup>a</sup> Different types. <sup>b</sup> Value in parenthesis gives the number of interactions of each types per molecule

on the basis of HS analysis for all the compounds is shown in Fig. 9.

## EXPERIMENTAL

### Materials and methods

All the chemicals employed here for the synthesis were commercially available reagents of analytical grade and were used without further purification. Solvents used for the synthesis were purified using the available literature methods [17].

### Synthesis of 5,10,15,20-tetratolylporphyrin, its metal complexes and 2,3,12,13-tetrabromo-5,10,15,20-tetratolylporphyrin

5,10,15,20-tetratolylporphyrin, H<sub>2</sub>TTP ligand, **1**, was prepared using Adler–Longo method.

(Note: we used propionic anhydride in place of propionic acid while refluxing it by which the excess moisture content present in the acid can be removed). The antipodal β-pyrrole bromination of **1** was done using the modified literature method [10]. Chloroform solution of **1** was stirred and refluxed with 6 equivalents of freshly recrystallized *N*-bromosuccinimide (NBS) and the reaction was monitored with TLC and UV-visible spectroscopy. After 2 h of time, excess 4 equivalents of NBS was added and no lower brominated products were found. The tetrabrominated product, **2** is confirmed by UV-visible spectroscopic analysis comparing it with the antipodal brominated product of *meso*-tetraphenylporphyrin (H<sub>2</sub>TPPBr<sub>4</sub>). The resulting product (**2**) was dried and washed twice with methanol and purified by column chromatography followed by recrystallization in chloroform/methanol solution. The recrystallized product **2** was found

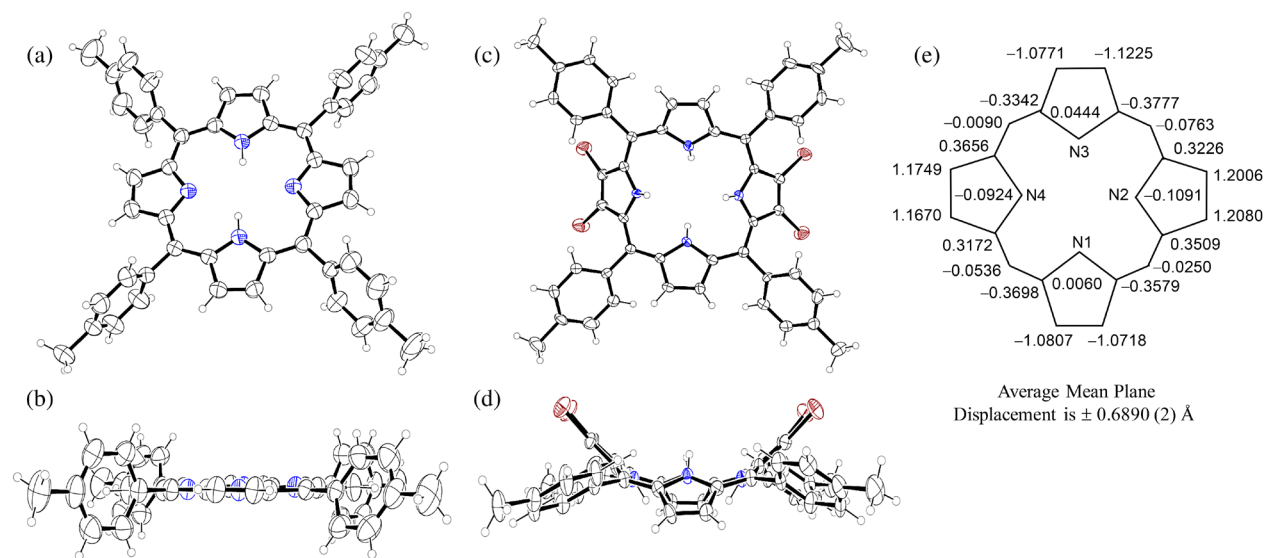


**Fig. 3.** ORTEP diagrams, (a, c) top and (b, d) side-on view of **1** and **2** (solvent molecules and disordered components removed for clarity and shown in 40% probability ellipsoids); and (e) average mean plane displacement of all atoms in **2** molecule

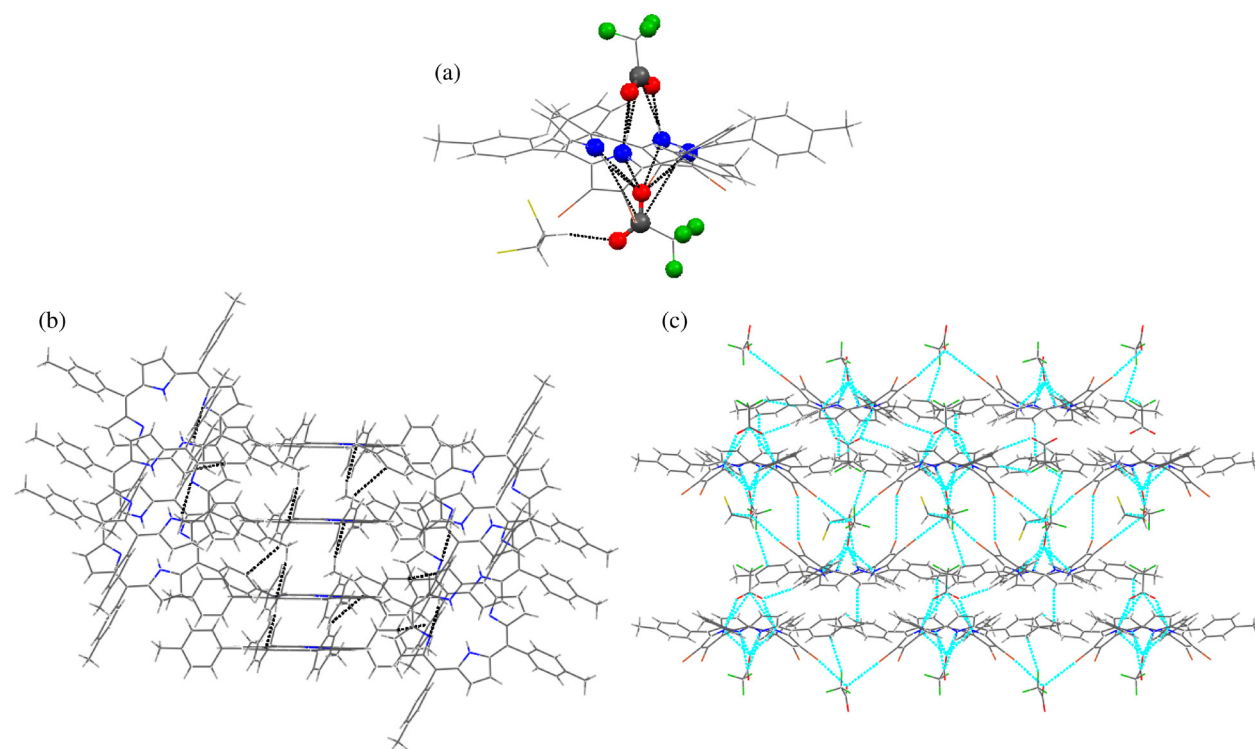


**Fig. 4.** (a) Wireframe structure of **2** with  $\text{CF}_3\text{COO}^-$  anions and a dichloroethane molecule indicating various intermolecular interactions, color scheme: grey-carbon, blue-nitrogen, red-oxygen, green-fluorine, brown-bromine, yellow-chlorine; (b) orthogonal arrangement of **1** viewed along 'bc' plane lead to form a one dimensional array; (c) slip-stack or off-set arrangement of **2** viewed down 'a' axis through various intermolecular interactions

to be poorly soluble in chlorinated solvents, and hence trifluoroacetic acid is used for crystallization which yields the diprotonated product,  $\text{H}_4\text{TTPBr}_4^{2+}(\text{CF}_3\text{COO})_2(\text{C}_2\text{H}_4\text{Cl}_2)$  (Note: NBS was purified as

per the literature method). The metal complexes of **3–5** were prepared by the literature method [11] to afford the desired complexes, yielded in 75–96% (Scheme 1). Manganese metalation was performed by treating **2** with

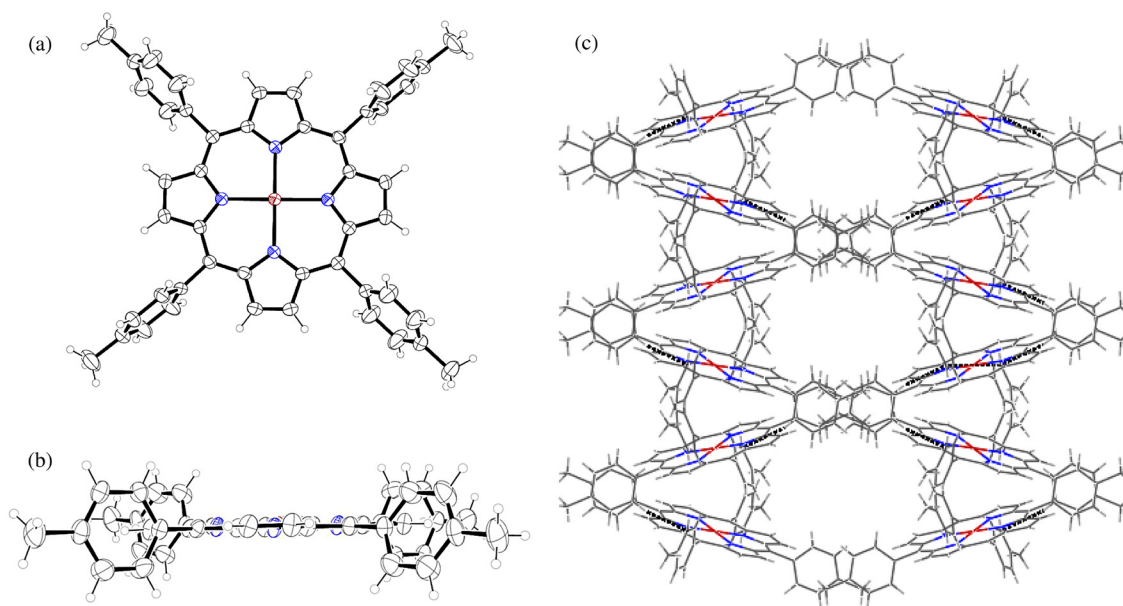


**Fig. 5.** ORTEP diagrams (a) top and (b) side-on view of **3**; (c) zigzag arrangement of **3** formed through  $(\text{ph})\text{C}\cdots\text{H}\cdots\text{C}(\text{ph})$  and  $(\text{ph})\text{C}\cdots\text{C}(\text{ph})$  interactions viewed down along 'ab' plane

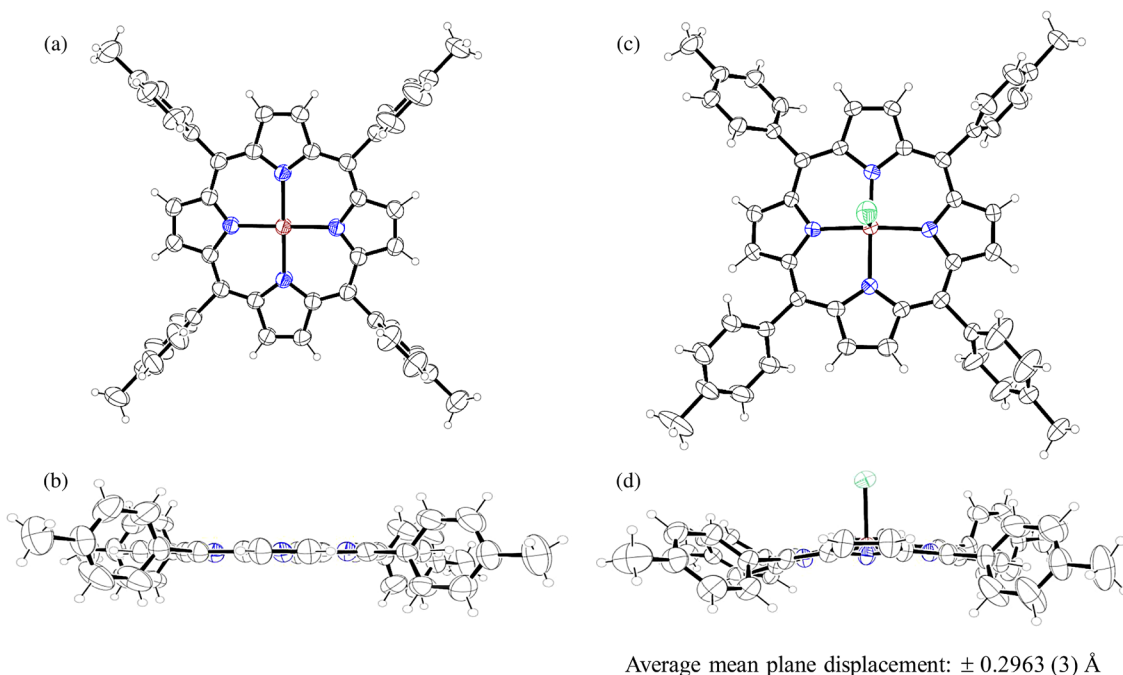


**Fig. 6.** ORTEP diagrams, (a, c) top and (b, d) side-on view of **4** and **5** (solvent molecules and disordered components removed for clarity and shown in 40% probability ellipsoids)

$\text{Mn}^{\text{II}}\text{Cl}_2$  in *N,N*-dimethylformamide in presence and absence of nitrogen atmosphere, resulted the formation of  $\text{Mn}^{\text{II}}\text{TTP}$  and  $\text{Mn}^{\text{III}}\text{TTPCl}$  respectively.

### X-ray structure determination

Single crystal X-ray diffraction data of **1–5** were collected by the selection of appropriate suitable single crystals which are formed by the vapor diffusion method

using appropriate solvent systems. All the crystals were grown at room temperature and single crystal X-ray structure data collections were performed on a Bruker AXS Kappa Apex II CCD diffractometer with graphite monochromated  $\text{Mo K}\alpha$  radiation ( $\lambda = 0.71073 \text{ \AA}$ ). Crystals were coated with paraffin oil (inert), mounted on a fibre capillary and data were collected at 273 K. The reflections with  $I > 2\sigma(I)$  were employed for structure solution and refinement. The SIR92 [18] (WINGX32)

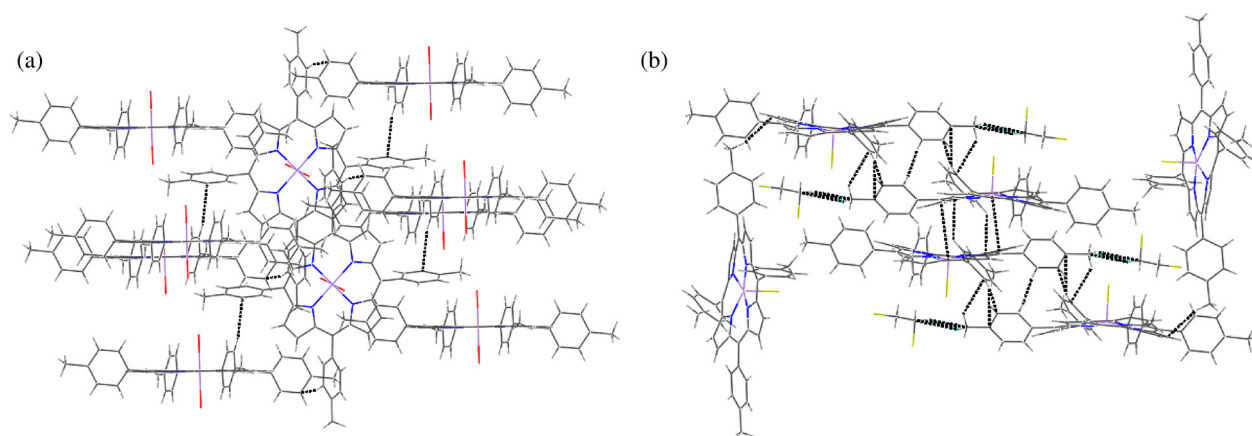


**Fig. 7.** (a) Orthogonal arrangement of **4** through  $(\text{ph})\text{C-H}\cdots\text{C}(\text{ph})$  interaction viewed along 'bc' plane; (b) slip-stack or off-set fashion of **5** viewed down 'a' axis

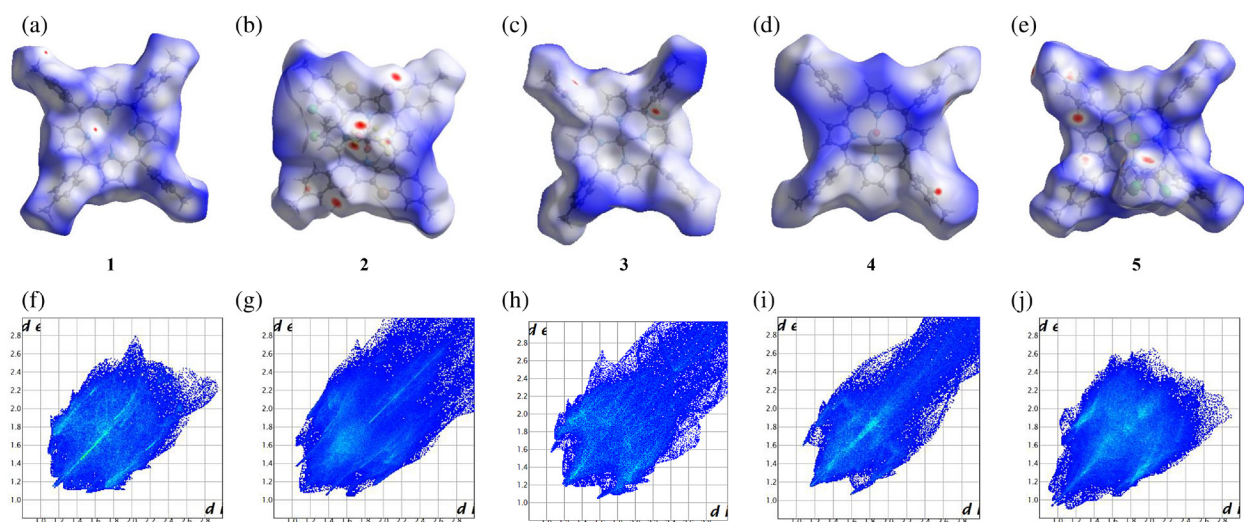


**Fig. 8.** (a) Hirshfeld surfaces mapped with (a–e)  $d_{\text{norm}}$  ranging from  $-0.40 \text{ \AA}$  (red) to  $2.50 \text{ \AA}$  (blue); (f–j) 2D fingerprint plots with  $d_i$  and  $d_e$  ranging from  $1.0$  to  $2.8 \text{ \AA}$  for **1–5**

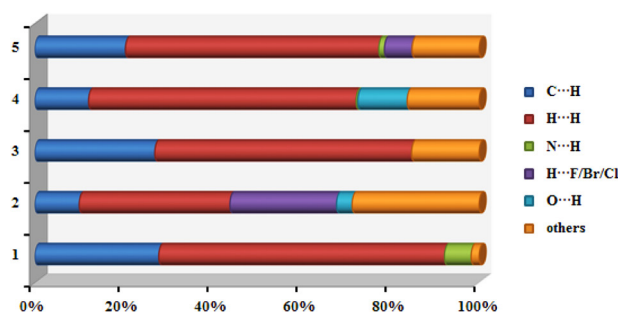


**Fig. 9.** Percentage distribution of individual intermolecular interactions on the basis of Hirshfeld surface analysis of **1–5**

program was used for solving the structure by direct methods. Successive Fourier synthesis was employed to complete the structures after full-matrix least squares refinement on  $|F|^2$  using the SHELXL97 [19] software.

Fourier syntheses led to the location of all of the non-hydrogen atoms. For the structure refinement, all data were used including negative intensities. The criterion of  $F^2 > 2\sigma(F^2)$  was employed for calculating  $R_1$ .  $R$  factors based on  $F^2(wR_2)$  are statistically about twice as large as those based on  $F$ , and  $R$  factors based on all data will be even larger. Non-hydrogen atoms were refined with anisotropic thermal parameters. All of the hydrogen atoms in the porphyrin structure could be located in the difference map. However, the hydrogen atoms were geometrically relocated at chemically meaningful positions and were given riding model refinement.

### Hirshfeld surface analysis

We analyzed the crystal structures by Hirshfeld surface analysis (HSs) and 2D fingerprint plots (FPs) using *Crystal Explorer 3.1* [16] based on results of

single crystal X-ray diffraction studies. The function  $d_{\text{norm}}$  is a ratio of distances of any surface point to the nearest interior ( $d_i$ ) and exterior ( $d_e$ ) atom and the van der Waals radii of the atoms [20]. The negative value of  $d_{\text{norm}}$  indicates the sum of  $d_i$  and  $d_e$  is shorter than the sum of the relevant van der Waals radii, which is considered to be a closest contact and is envisaged by the red color in the Hirshfeld surfaces. The white color denotes intermolecular distances close to van der Waals contacts with  $d_{\text{norm}}$  equal to zero whereas contacts longer than the sum of van der Waals radii with positive  $d_{\text{norm}}$  values are colored with blue. A plot of  $d_i$  vs.  $d_e$  is a 2D fingerprint plot which recognizes the existence of different types of intermolecular interactions.

## CONCLUSION

In summary, we performed the structural elucidation and study of various intermolecular interactions of *meso*-tetratolylporphyrins, **1–5** using single crystal X-ray diffraction studies combined with computational Hirshfeld surface analysis. Our results reveal that the planar systems, **1**, **3** and **4** are packed in a “orthogonal fashion” possessing intermolecular interaction mainly of  $(\text{ph})\text{C}-\text{H}\cdots\text{C}(\text{ph})$  which is in the range of  $\sim 2.81$  Å whereas the crystal packing of non-planar systems, **2** and **5** in a “slip-stack or off-set fashion” through various intermolecular interactions. The non-planar porphyrin, **2** exhibits saddle geometry whereas **5** showed a domed geometry as evident from the single crystal X-ray diffraction studies. The enhancement of non-planarity in **2** is presumably due to the presence of various intermolecular interactions caused by the presence of  $\text{CF}_3\text{COO}^-$  anions on both faces of the porphyrin in addition to the bulky bromine groups at the  $\beta$ -pyrrole positions. In **5**, the non-planarity is merely due to the metal coordination at the porphyrin core as pentacoordinated  $\text{Mn}^{\text{III}}$  centre with a chloro ligand in the axial position. The Hirshfeld surface analysis of porphyrins **1–5** indicates that the crystal packing is mainly stabilized by the close contacts involving  $\text{C}\cdots\text{H}$  [28% in **1**; 26% in **3**; 12% in **4**] and  $\text{H}\cdots\text{H}$  [64% in **1**; 48% in **3**; 52% in **4**] in planar porphyrins; whereas in non-planar porphyrins, in addition to the above major interactions, the close contacts involving halogens  $\text{H}\cdots\text{F}/\text{Cl}/\text{Br}$  [24% in **2**; 15% in **5**] also play a major role in the formation of supramolecular network.

## Acknowledgements

Financial support from DST, New Delhi to CA (SB/EMEQ-016/2013) is gratefully acknowledged. We would like to thank Dr. Babu Varghese, SAIF, IIT Madras for the single crystal data collection, structure solution and refinement.

## Supporting information

Crystallographic data for porphyrins **1–5** have been deposited at the Cambridge Crystallographic Data Center

(CCDC) under numbers CCDC-1041763, 956522, 1058016, 1041764 and 980778. Copies can be obtained on request, free of charge, via [www.ccdc.cam.ac.uk/data\\_request/cif](http://www.ccdc.cam.ac.uk/data_request/cif) or from the Cambridge Crystallographic Data Center, 12 Union Road, Cambridge CB2 1EZ, UK (fax: +44 1223-336-033 or email: [data\\_request@ccdc.cam.ac.uk](mailto:data_request@ccdc.cam.ac.uk)).

## REFERENCES

- Milgrom LR. *The colors of life: An introduction to the chemistry of porphyrins and related compounds*, Oxford University Press: New York, 1997.
- Senge MO. In *The Porphyrin Handbook*, Vol. 1, Kadish KM, Smith KM and Guillard R. (Eds.), Academic Press: San Diego, CA, 1999; p. 239.
- Shelnutt JA, Song X-Z, Ma J-G, Jia S-L, Jentzen W and Medforth CJ. *Chem. Soc. Rev.* 1998; **27**: 31–42 and references therein.
- Sheldon RA. *Metalloporphyrins in Catalytic Oxidations*, Marcel Dekker Inc: New York, 1994.
- Parusel ABJ, Wondimagegn T and Ghosh A. *J. Am. Chem. Soc.* 2000; **122**: 6371–6374.
- Song X-Z, Jentzen W, Jia S-L, Jaquinod L, Nurco DJ, Medforth CJ, Smith KM and Shelnutt JA. *J. Am. Chem. Soc.* 1996; **118**: 12975–12988.
- Senge MO, Ema T and Smith KM. *J. Chem. Soc., Chem. Commun.* 1995; 733–734.
- (a) Sujatha S and Arunkumar C. In *Fluorinated Porphyrinic Crystalline Solids: Structural Elucidation and Study of Intermolecular Interactions, Crystalline and Non-crystalline Solids*, Mandracci P. (Ed.) InTech Publishers: (ISBN 978-953-51-4721-3) — Open Science Open Minds, 2016; ch. 4, pp. 57–78. (b) Soman R, Sujatha S, De S, Rojisha VC, Parameswaran P, Varghese B and Arunkumar C. *Eur. J. Inorg. Chem.* 2014; 2653–2662. (c) Soman R, Sujatha S and Arunkumar C. *J. Fluor. Chem.* 2014; **163**: 16–22. (d) Kooriyaden FR, Sujatha S, Varghese B and Arunkumar C. *J. Fluor. Chem.* 2015; **170**: 10–16.
- Lindsey JS, Schreiman IC, Hsu HC, Kearney PC and Marguerettaz AM. *J. Org. Chem.* 1987; **52**: 827–836.
- (a) Callot HJ. *Tetrahedron Lett.* 1973; **14**: 4987–4990. (b) Callot HJ. *Bull. Soc. Chim. Fr.* 1974; **7–8**: 1492. (c) Crossley MJ, Burn PL, Chew SS, Cuttance FB and Newsom IA. *J. Chem. Soc. Chem. Commun.* 1991; 1564–1566. (d) Terazono Y, Patrick BO and Dolphin DH. *Inorg. Chem.* 2002; **41**: 6703–6710. (e) Kumar PK, Bhyrappa P and Varghese B. *Tetrahedron Lett.* 2003; **44**: 4849–4851. (f) Bhyrappa P, Velkannan V, Karunanithi K, Varghese B and Harikrishna. *Bull. Chem. Soc. Jpn.* 2008; **81**: 995–1001.
- Adler AD, Longo FR, Kampas F and Kim J. *J. Inorg. Nucl. Chem.* 1970; **32**: 2443–2445.

12. Bhyrappa P, Arunkumar C and Varghese B. *Acta Cryst.* 2008; **C64**: o276–o278.
13. (a) Dastidar P and Goldberg I. *Acta Cryst.* 1996; **C52**: 1976–1980. (b) McGill S, Nesterov VN and Gould SL. *Acta Cryst.* 2010; **E66**: m723.
14. Scheidt WR, Mondal JU, Eigenbrot CW, Adler A, Radonovich LJ and Hoard JL. *Inorg. Chem.* 1986; **25**: 795–799.
15. (a) Bhyrappa P, Arunkumar C and Vittal JJ. *J. Chem. Sci.* 2005; **117**: 139–143 and references cited therein. (b) Schauer CK, Anderson OP, Eaton SS and Eaton GR. *Inorg. Chem.* 1985; **24**: 4082–4086.
16. Wolff SK, Grimwood DJ, McKinnon JJ, Turner MJ, Jayatilaka D and Spackman MA. Crystal Explorer 3.1 (2013), University of Western Australia, Crawley, Western Australia, 2005–2013; <http://hirshfeldsurface.net/CrystalExplorer>.
17. Perrin DD and Armarego WLF. *Purification of organic solvents*, Pergamon Press: Oxford, 1988.
18. Altomare AG, Cascarano G, Giacovazzo C and Gualardi A. *J. Appl. Crystallogr.* 1993; **26**: 343–350.
19. Sheldrick GM, SHELXL97; University of Goettingen: Goettingen, Germany, 1997.
20. (a) Hirshfeld FL. *Theor. Chim. Acta* 1977; **44**: 129–138. (b) Spackman MA and McKinnon JJ. *CrystEngComm.* 2002; **4**: 378–392. (c) Spackman MA and Jayatilaka D. *CrystEngComm.* 2009; **11**: 19–32.